Fluid acceleration effects on suspended sediment transport in the swash zone

J. A. Puleo, K. T. Holland, and N. G. Plant
Naval Research Laboratory, Stennis Space Center, Mississippi, USA

D. N. Slinn and D. M. Hanes[1]
Civil and Coastal Engineering Department, University of Florida, Gainesville, Florida, USA

Received 1 May 2003; revised 28 July 2003; accepted 3 September 2003; published 13 November 2003.

[1] Suspended sediment concentrations and fluid velocities measured in the swash zone of a high-energy steep beach were used to investigate the importance of fluid accelerations to suspended sediment transport. Swash flow acceleration was nearly constant at about one-half downslope gravitational acceleration with two important exceptions. We observed strong, short-lived periods of accelerating uprush at the beginning of the swash cycle and decelerating backwash at the end of the swash cycle (magnitudes of both approximately twice that of the expected downslope gravitational acceleration). Interestingly, spikes in suspended load followed the anomalies in acceleration in a way that was not apparent from the nearly symmetric (in magnitude) ensemble averaged velocity time series. Suspended load values were largest during accelerating uprush associated with the shoreward propagating turbulent bore or swash front. During backwash, suspended loads were generally not as large. Correspondingly, suspended sediment transport rates obtained from the sediment concentration and velocity measurements showed best comparisons with a modified sediment transport model that includes a physical mechanism for enhancing transport rates due to flow acceleration. The modified sediment transport model reduced the overall root-mean square prediction error by up to 35% and shifted the predicted peak in uprush sediment transport rate earlier in the swash cycle, resulting in a better fit to the observations. These findings suggest that the inclusion of the acceleration term may account for physical mechanisms that include bore turbulence and horizontal pressure gradients typically associated with the accelerating portion of uprush. *INDEX TERMS:* 4546 Oceanography: Physical: Nearshore processes; 4558 Oceanography: Physical: Sediment transport; 3020 Marine Geology and Geophysics: Littoral processes; *KEYWORDS:* uprush, swash zone bore, turbulence, pressure gradient

Citation: Puleo, J. A., K. T. Holland, N. G. Plant, D. N. Slinn, and D. M. Hanes, Fluid acceleration effects on suspended sediment transport in the swash zone, *J. Geophys. Res.*, *108*(C11), 3350, doi:10.1029/2003JC001943, 2003.

1. Introduction

[2] The swash zone is one of the most scientifically challenging oceanic environments for describing sediment transport. Here, uprush and backwash motions mobilize and transport large quantities of sediment compared to other regions [e.g., *Beach and Sternberg*, 1991; *Hughes et al.*, 1997; *Masselink and Hughes*, 1998; *Butt and Russell*, 1999; *Osborne and Rooker*, 1999 and *Puleo et al.*, 2000]. Gradients in the relatively small time-integrated transport drive morphological change. In order to predict changes in beach morphology, an understanding of the physical processes is needed to develop an accurate mathematical description of sediment transport mechanisms in the swash zone.

[3] Sediment transport in the swash zone has generally been described with an energetics-type formulation originally derived by *Bagnold* [1966] for steady unidirectional flows and later adapted by *Bowen* [1980] and *Bailard* [1981] (hereinafter referred to as B3 models) for time-dependent flows and used in several studies [e.g., *Hardisty et al.*, 1984; *Hughes et al.*, 1997; *Masselink and Hughes*, 1998; *Puleo et al.*, 2000]. Although the range of observations supporting these descriptions in the swash zone is somewhat limited, B3-type relationships have occasionally shown some significant correlation between predicted and measured sediment transport rates [e.g., *Masselink and Hughes*, 1998]. In addition, several studies have modified the original B3 equations in the hope of increasing the

[1]Also at U.S. Geological Survey Pacific Science Center, Santa Cruz, California, USA.

0148-0227/03/2003JC001943$09.00

predictive skill at matching measurements. For instance, *Puleo and Holland* [2001] and *Butt et al.* [2001] have suggested that the friction coefficient, f, varies between uprush and backwash and may even be a function of water depth. Since B3 models depend linearly on f, inclusion of this uprush-backwash variation could lead to improvement of sediment transport predictions either directly or indirectly by accounting for unrelated physical processes.

[4] The B3 type models rely on velocity moments and hence do not explicitly account for flow unsteadiness that has been shown to affect boundary layer structure and hence energy dissipation at the bed. An example was given by *King* [1991] who showed that the boundary layer development is slowed in an accelerating flow, implying the thickness is less than that for a steady flow (further described by *Nielsen* [1992]). The delayed development is easily understood for a laminar flow where rapid velocities may remain closer to the bed than in steady flow thereby increasing the bed shear stress. This explanation is less clear in a fully turbulent boundary layer where more mixing is likely to occur. Also, there is a phase lag between the free stream velocity and that in the boundary layer. These unsteady boundary layer effects are not incorporated into the B3 models, even though they appear to have a significant influence on sediment transport [e.g., *Hanes and Huntley*, 1986; *Jaffe and Rubin*, 1996]. For instance, *Drake and Calantoni* [2001] adapted a sheet flow model and added an extra term to the B3 bed load formula to account for acceleration effects (manifested through horizontal pressure gradients). Their numerical results showed that the inclusion of acceleration effects significantly improved the skill of the sediment transport model. Fluid accelerations have also been related to sandbar morphology [*Elgar et al.*, 2001; *Hoefel and Elgar*, 2003] where it was shown that the peak in acceleration skewness of surf zone flows was well correlated to onshore sandbar motion. *Admiraal et al.* [2000] developed relationships based on fluid accelerations and sediment response to predict the phase lag between maximum shear stress and peak suspended sediment concentrations from laboratory measurements in a flume.

[5] While several studies have addressed the effect of fluid acceleration either from a theoretical viewpoint or for the surf zone, fewer studies have applied these concepts to the swash zone. *Nielsen* [2002] adopted the *Meyer-Peter and Muller* [1948] sediment transport model for swash by including a phase shift in the shear stress term. This phase shift accounts for greater bed shear stresses for a given velocity during accelerating flow. In the swash zone, this is most important to the accelerating portion of the uprush where peak velocities are higher and sediment tends to be more concentrated than during backwash [e.g., *Butt and Russell*, 1999; *Puleo et al.*, 2000]. In fact, *Butt and Russell* [1999] used field data to show that sediment suspension events coincided with periods of large onshore-directed fluid acceleration.

[6] The primary aim of this study is to describe the link between fluid acceleration and sediment transport in the swash zone, using field observations from a natural beach. The secondary aim is to use the new understanding of swash zone sediment transport to make a modification to the B3 model and to test this modification. Section 2 describes the expected fluid motions based on idealized models. The B3-type sediment transport equation and the modification caused by including acceleration are presented in section 3. Section 4 briefly describes the field set up and data collected. Observations of suspended loads in velocity-acceleration space and comparisons between observations and model predictions are given in section 5. Discussion and conclusions are given in sections 6 and 7, respectively.

2. Idealized Swash Motions and Sediment Transport

[7] Before developing the acceleration-based modification for the swash zone application of the Bailard model, it is important to understand the context to which this acceleration may play a role in swash zone suspended sediment transport. Technically, the swash motion begins after bore collapse into very shallow water [O(mm - cm)] or exposed (possibly wetted) bed. The inertia of the shoaling wave and the pressure force from the collapse accelerate the mass of water up the beach face. Toward the end of the backwash the seaward directed flow collides with the next incident bore (decelerates) leading to the ensuing swash event.

[8] Frictional ballistic motion often applied to describe the swash cycle [*Ho and Meyer*, 1962; *Shen and Meyer*, 1963 and *Kirkgöz*, 1981] balances fluid acceleration against gravity and friction (see *Puleo and Holland* [2001] for analytic formulation). An example showing a Lagrangian velocity and acceleration time history for the leading edge and solely cross-shore flow is given in Figure 1 (defining the cross-shore direction, x, to be positive offshore). The flow is modeled analogous to a block moving up and down a frictional incline with a beach slope of 1:12, initial velocity, $u0$, of 4 m s^{-1}, friction factor of 0.01 and a leading edge water depth of 0.05 m. An instantaneous increase in velocity would be expected as the uprush begins, followed by uprush deceleration, flow reversal, and backwash acceleration during the seaward phase. Note also that the theory does not describe the swash motion before the leading edge reaches the collapse point such that it only applies just after uprush initiation and just before the next uprush starts. Throughout this paper, the term acceleration will be used to refer to a flow with increasing velocity magnitude. The term deceleration will only be used for referencing a flow whose rate of speed is decreasing. This is simpler terminology than using the term negative acceleration because in swash studies, fluid motions occur in both the positive and negative directions.

[9] The effect of friction is indicated in the velocity time series (Figure 1a) by the swash duration being shortened and by flow velocities nearly always being less than frictionless motion (after accounting for swash phase due to differences in duration). The figure shows that the flow is decelerating throughout uprush and accelerating throughout backwash (Figure 1b). Near the initiation of the swash motion, the flow decelerates faster than downslope gravitational acceleration, a_{grav}, because both gravity and friction forces are acting together against the flow in the downslope direction. Acceleration values are only close to a_{grav} during times of small fluid velocity when

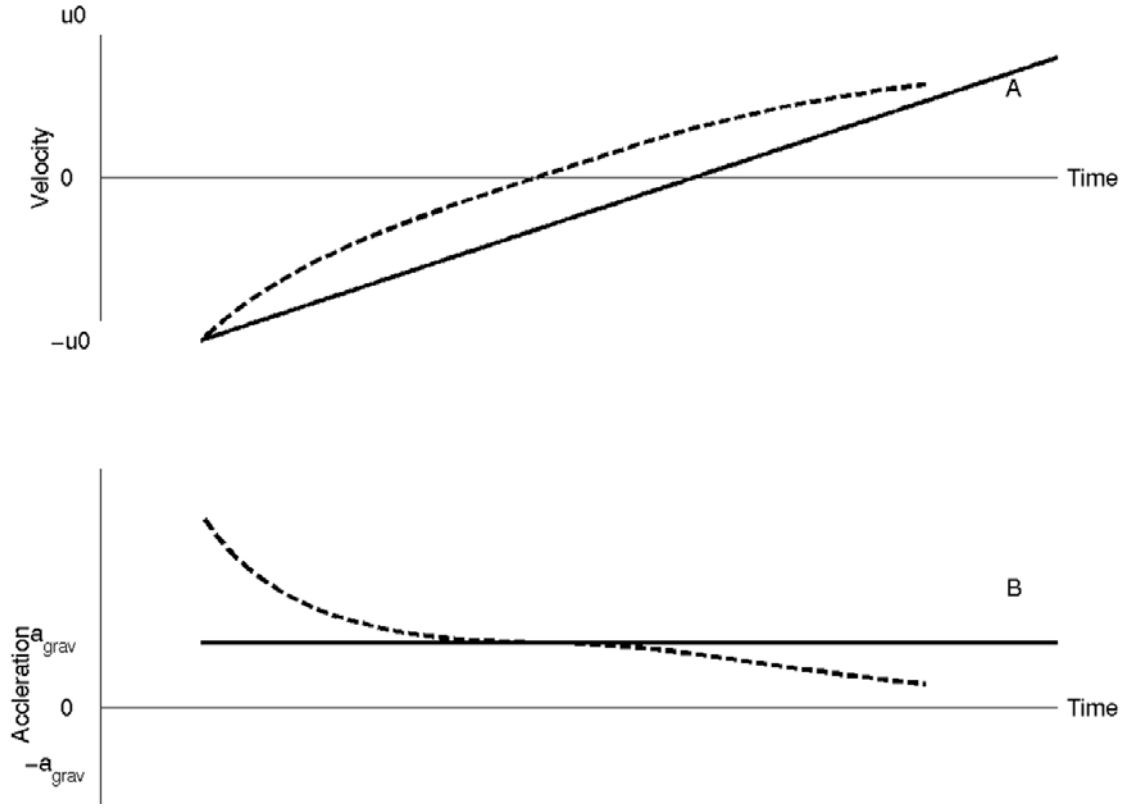

Figure 1. Theoretical ballistic motion for leading edge (a) velocity and (b) acceleration without (solid line) and with (dashed line) friction. The initial velocity, *u0*, is 4.0 m s^{-1} and a_{grav} is the downslope gravitational acceleration for a beach slope of 1:12. Inviscid swash duration is roughly 9.8 s.

the friction force is also small. After flow reversal, the acceleration is less than a_{grav} because friction and gravity forces are opposing each other. In short, the simple frictional theory for Lagrangian swash edge motion predicts a decelerating uprush and accelerating backwash during their respective cycles.

[10] While the Lagrangian description of leading edge fluid motion is often applied in the swash zone, observations of Eulerian swash motions sampled with a current meter may yield a different typical time series for the interior (behind the leading edge) flow (Figure 2, from ducted impellor current meter data [*Puleo et al.*, 2000], and similar to that used by *Nielsen* [2002]). Here the velocity does not increase instantaneously to its maximum, but does a short time after the sensor is inundated [e.g., *Nielsen*, 2002, Figure 2]. The inundation by swash at a given point represents a large onshore-directed acceleration (Figures 2a and 2b) as expected, but is not predicted by the simple ballistic model (which always predicts decelerating uprush flow). The swash flow then decelerates roughly according to gravity and friction (and likely horizontal pressure gradients). This is evident from Figure 2b where the acceleration curve approaches but does not quite reach downslope gravitational acceleration (denoted by dotted line). After flow reversal, the seaward-directed flow accelerates under gravity and friction, but does not continue to accelerate according to those processes alone, because the seaward flow is resisted by fluid mass offshore creating an adverse pressure gradient. Hence backwash flow is not entirely ballistic as offshore fluid levels cause deceleration in the backwash. This is evidenced in Figure 2b where the acceleration curve becomes negative while the flow velocity is still in the positive (offshore) direction. Because of this, the maximum observed backwash velocity within a single swash cycle may not occur at the last value recorded by the sensor (Figure 2a) except at times, when the sensor emerges from the water column. While this schematic may not apply to all natural swash events it does point to differences between Lagrangian and Eulerian velocity and acceleration time series.

[11] The differences mentioned above may have a potential effect on swash zone sediment transport. For instance, even though swash velocity time series can be roughly symmetric (Figure 2a and *Holland and Puleo* [2001]) or have slightly longer backwash durations with roughly equal velocity magnitudes [*Masselink and Hughes*, 1998], several studies have shown the dominance of suspended sediment during uprush [e.g., *Masselink and Hughes*, 1998; *Butt and Russell*, 1999; *Puleo et al.*, 2000]. Yet the rough velocity symmetry used in a velocity-based suspended sediment transport model with a bed slope effect would suggest continual foreshore erosion (same conclusion arrived at if a velocity-based bed load model is used). On the basis of these previous findings and because beaches cannot continually erode, another mechanism, not tied solely to velocity, should exist to balance this apparent deficiency in uprush transport. Large onshore-directed

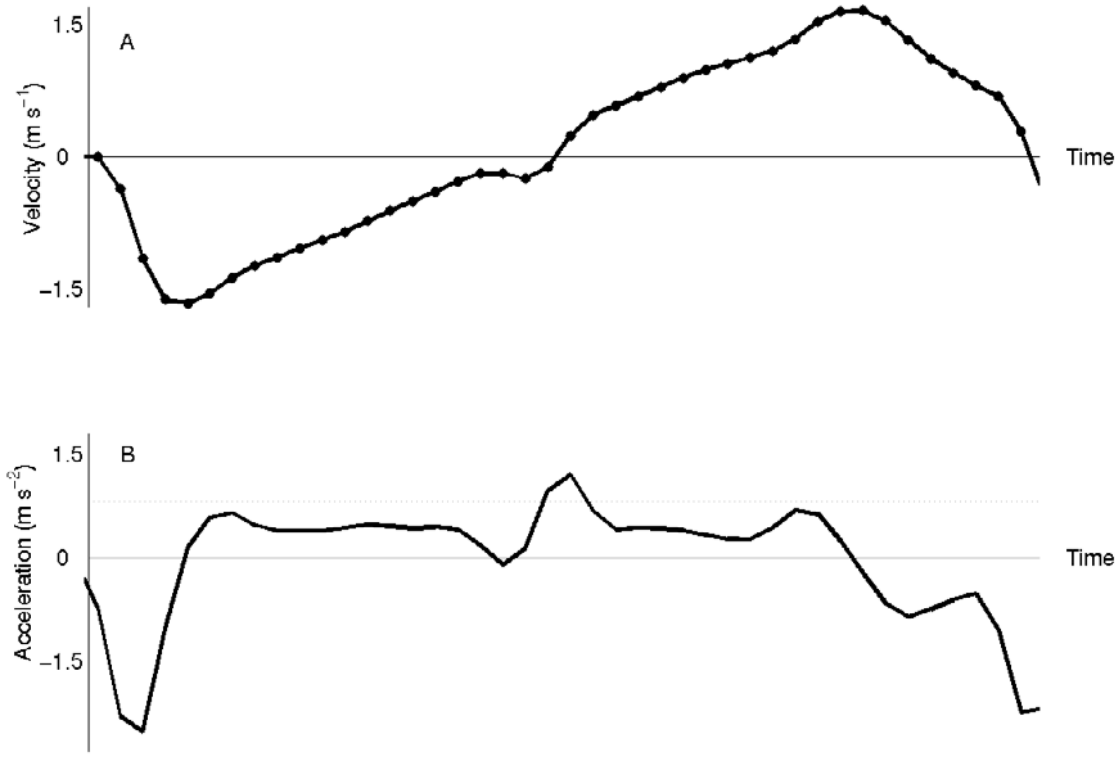

Figure 2. Swash schematic from current meter data showing (a) velocity and (b) acceleration profile. The solid horizontal lines represent zero velocity and acceleration. Dotted line in Figure 2b is downslope gravitational acceleration on a 1:12 sloping beach. Swash duration is roughly 10 s.

turbulence associated with the swash zone bore [*Butt and Russell*, 1999; *Puleo et al.*, 2000] is the likely mechanism and including the fluid acceleration, a potential proxy for this bore turbulence, in a sediment transport formulation may lead to improved predictions.

3. Suspended Sediment Transport Equations and the Development of the Acceleration Modification

[12] The *Bailard* [1981] suspended load formulation (hereinafter referred to as the Bailard model) relates the immersed weight suspended sediment transport to the fluid power as

$$q_B = K_d \omega_d = \frac{\varepsilon_s u}{w} \omega_d, \tag{1}$$

where q_B (kg s^{-3}) is the time-dependent immersed weight suspended sediment transport rate, u is the cross-shore velocity, ε_s is a suspended load efficiency, w is the sediment fall velocity, and ω_d is the local rate of energy dissipation per unit surface area (a portion of which is available to transport sediment), given by

$$\omega_d = \tau_d u. \tag{2}$$

Here τ_d is the bed shear stress and can be expressed by a quadratic drag law

$$\tau_d = \frac{1}{2} \rho f |u| u, \tag{3}$$

where ρ is the fluid density and f is an empirical friction factor. Incorporating equation (3) into equation (1) leaves

$$q_B = \frac{\varepsilon_s \rho f}{2w} u|u|^3 = ku|u|^3. \tag{4}$$

Note that in this formulation we have not included the downslope term as it has been previously disregarded in sediment transport studies in the swash zone [e.g., *Hughes et al.*, 1997; *Masselink and Hughes*, 1998] and shown to be minimal in predictions of sandbar motion [*Thornton et al.*, 1996; *Gallagher et al.*, 1998].

[13] Since arguments given in section 2 suggested that sediment transport may depend on acceleration, a simple modification will be made to equation (4) to incorporate acceleration effects. Furthermore, since the Bailard model given here is time dependent it is consistent to use an acceleration modification that may also be time dependent unlike the acceleration skewness proposed by *Drake and Calantoni* [2001] and *Elgar et al.* [2001] that are statistics derived from a velocity time series but cannot be used to investigate the phase-dependent nature of swash zone sediment transport.

[14] The effect of fluid acceleration on sediment transport is not well understood, but thought to alter the force on the bed through strong horizontal pressure gradients [e.g., *Drake and Calantoni*, 2001] (parameterized through fluid accelerations). The total force on sediment particles on the bed can, therefore, be recast to include parameterizations of drag and inertia forces (the latter containing acceleration). The drag

force on a sand grain and that extrapolated to the bed are both given through a quadratic drag law. In a crude manner, we also assume the inertial forces on a sand grain can be similarly extrapolated to the bed yielding a combined force as

$$F = F_d + F_p = \frac{1}{2}\rho f|u|uA + \rho V k_m a, \quad (5)$$

where A is the bed surface area, V is the volume, a is the local fluid acceleration, and k_m is a constant coefficient. The convective acceleration, normally included in the inertia force, has not, to our knowledge, been studied in the swash zone, but future work may show its importance. It is excluded in this formulation since field measurements were obtained from only a single location in the cross-shore (see section 4). Furthermore, particle intergranular forces normally included in sediment transport models that operate at the particle scale are not included here. The intent is to use a simple approach guided by some physical justification to determine the form of the acceleration term for the ''macro'' scale affect of acceleration on sediment transport akin to the drag-law-driven energetics approach that is similarly focused on predicting bulk sediment transport rather than grain-to-grain interactions and individual particle motions. If one wishes, the acceleration modification in equation (5) can be viewed similarly to the pressure gradient force extension used in the *Drake and Calantoni* [2001] model, but for instantaneous rather than time averaged transport predictions.

[15] The total shear stress is then given by the total force per unit area of bed as

$$\tau = \frac{1}{2}\rho f|u|u + \rho k_m d a, \quad (6)$$

whereupon division by the surface area, A, a vertical length scale, d, is needed. If the length scale is assumed to be constant, then the logical choice for the length scale when applied to a single grain is the grain diameter. It is not clear, however, that the grain diameter is the appropriate length scale in this formulation for shear stress and hence it should not be assumed that the inertia force is negligible when applied to the bed. Regardless, a constant length scale would become incorporated into the leading coefficient and would not need to be specified a priori. If, on the other hand, one assumes that the acceleration in the swash zone is largely associated with the turbulent leading edge and bore [*Butt and Russell*, 1999], then a logical choice for the length scale would be the water depth since the turbulence is able to extend from the water surface to the bed [*Petti and Longo*, 2001, *Cowen et al.*, 2003]. For the time being, the model will, for simplicity, include the length scale in the leading coefficient (assumes a constant value). Variations arising from using the time-dependent water depth, however, will be mentioned in the results section.

[16] Using equation (6) for the bed shear stress, a new formulation for suspended sediment transport becomes

$$q_{pred} = k_b u|u|^3 + k_a|u|^2 a, \quad (7)$$

where subscripts b and a represent coefficients for the Bailard model and the added acceleration effect, respectively. Throughout this paper, equation (7) will be referred to as the modified model. Transport relationships like equation (7) are often utilized in a time-averaged form such that a transport rate is determined per swash cycle or for a length of time series. Time averaging erases all phase information. In this study, we are interested in the phase-dependent nature of sediment transport throughout a swash cycle and will use ensemble averages of swash events instead.

4. Field Study

[17] Data were collected at Gleneden Beach, Oregon, in February 1994. This beach is intermediate to steep with a foreshore beach slope of roughly 1:12 and a median grain size of 0.44 mm. Complete details of the data collection, reduction, and experimental setup are given by *Puleo et al.* [2000]. Briefly, two ducted impellor current meters (initially 4 and 8 cm above bed), a pressure sensor (initially at bed level), and a fiber optic backscatter system (FOBS) to measure suspended sediment concentrations (penetrates the bed so that bed level and suspension concentration to within 1 cm of the bed can be obtained) were deployed at three locations on the foreshore separated by 5 m in the cross-shore direction.

[18] Data used in this study were obtained from the most landward location on February 27, 1994, and were collected during a high tide cycle (data from the other two locations on this day were not utilized due to intermittent current meter difficulty). Only several centimeters of bed level change occurred over the course of the run at this location. While the original sampling rate was 16 Hz, data were subsequently block averaged to 4 Hz to reduce noise. A 4-min time series on the rising tide is shown in Figure 3. Discontinuities in the η time series (Figure 3a) show that during this portion of the run, the sensors were intermittently immersed. The lower current meter velocity (Figure 3b) can be seen to increase rapidly (onshore is negative due to coordinate system), but as stated earlier, the increase is not always instantaneously to a maximum. At times, the velocity reaches the current meter maximum threshold of ± 1.67 m s^{-1}. Swash events containing velocities beyond this artificial cutoff will be excluded in all forthcoming analyses. The fluid acceleration, a (Figure 3c), was determined by a centered difference approximation using the measured velocity time series. Figure 3d shows that the estimate of the horizontal pressure gradient (using Taylor's hypothesis),

$$P = -g\frac{\partial \eta}{\partial x} = \frac{1}{u} g \frac{\partial \eta}{\partial t}, \quad (8)$$

is onshore during the entire swash event but strongest near the beginning of uprush and end of backwash. Equation (8) is only a rough estimate of the true horizontal pressure gradient because it inherently assumes that velocities are steady over the 0.5-s time period for which the value is calculated. This assumption may be violated at times in the swash zone where flows are expected to be highly variable. Taylor's hypothesis, however, has been used in previous swash studies [*Puleo et al.*, 2000] and for theoretical descriptions of bores and hydraulic jumps [*Johnson*, 1997]. Also, the use of the fluid velocity rather than wave celerity in equation (8) is more appropriate because within the swash zone, after bore collapse, the flow no longer represents a combined longitudinal/transverse wave or bore that would be observed farther seaward. Hence the concept

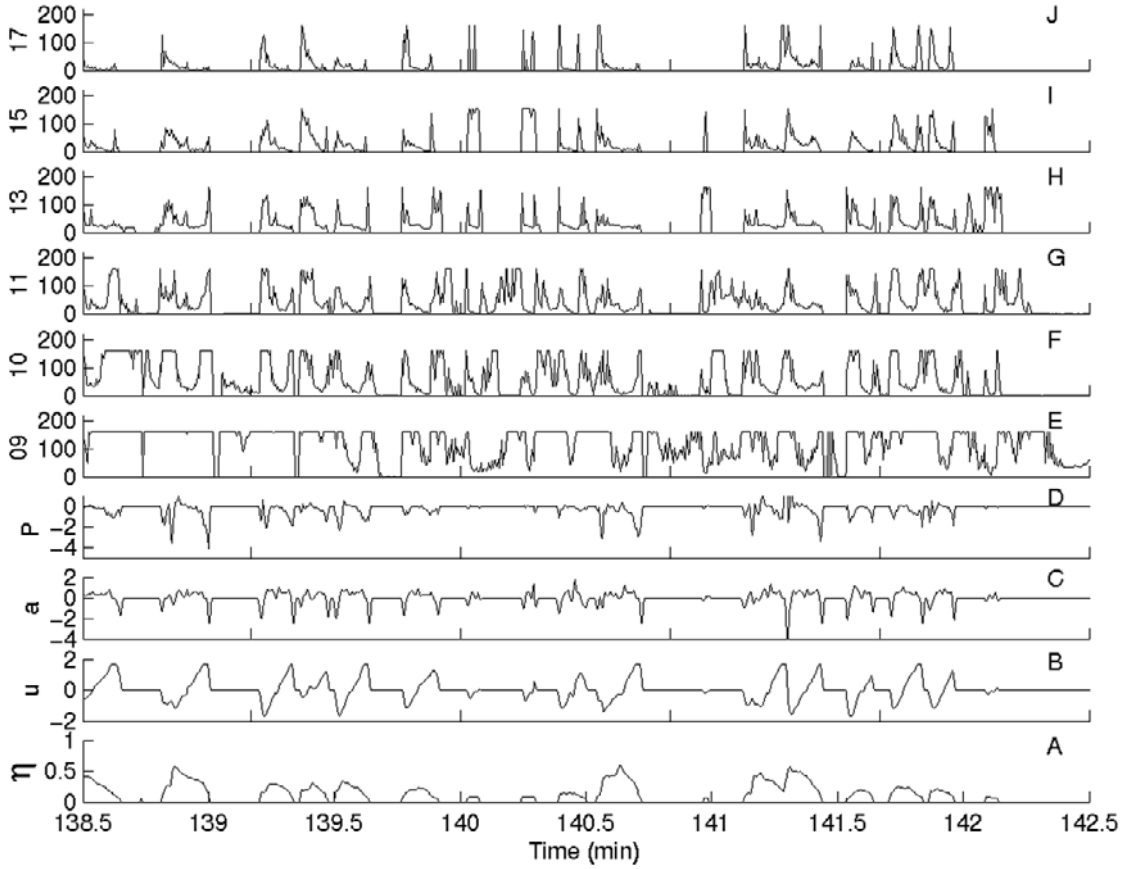

Figure 3. Four-minute swash time series. (a) Sea surface (m). (b) Swash zone fluid velocity (m s^{-1}) at 4 cm above the bed. (c) Swash zone fluid acceleration (m s^{-2}). (d) An estimate of the horizontal pressure gradient, P (m s^{-2}). (e–j) Suspended sediment concentration output from FOBS (g L^{-1}). Number on y axis is FOBS sensor number. The bed level is roughly at sensor 09 for this section of time series.

of wave celerity for true swash flows is no longer applicable and the use of u is more appropriate.

[19] The correspondence in Figures 3c and 3d imply that the fluid acceleration may also serve as a surrogate for the pressure gradient estimate. Suspension pulses tend to occur during sudden onshore-directed acceleration events as the swash reaches the sensors and during decelerating backwash. Individual suspension pulses (Figures 3e–3j) can be seen with the passing of each swash event. The suspension pulses extend at least 10 cm into the water column and likely higher for some swash events. The suspension data indicate that more sediment is generally carried as suspended load during the uprush than during the backwash as evidenced by the often asymmetric suspension peaks.

5. Results

5.1. Suspended Sediment Transport Calculation

[20] Dry mass suspended sediment loads, C, were calculated by taking the vertical integral of the suspended sediment concentration time series. The integral was carried to the water surface or to the highest FOBS sensor if the water elevation was above the highest sensor. Potential error does exist in this calculation since suspended sediment above the highest sensor is not included in addition to any noise from the measuring devices including signal saturation.

[21] The measured instantaneous immersed weight sediment transport rate, q_{meas}, is determined from the calculated dry mass suspended load and fluid velocity as

$$q_{meas} = \frac{\rho_s - \rho}{\rho_s} guC, \tag{9}$$

where u is the lower current meter (used in all calculations), and ρ_s and ρ are the sediment and fluid densities, respectively. Since velocities are thought to be essentially depth uniform except for very close to the bed [e.g., *Petti and Longo*, 2001], then using a uniform velocity to calculate the suspended load transport rates will not introduce significant error into the calculation.

5.2. Ensemble-Averaged Swash Events

[22] The velocity, acceleration, pressure gradient estimate, suspended load, and sediment transport time series were separated into individual swash events based on zero crossings of the velocity record. Swash events with a current maximum less than the cutoff and durations greater than 4 s were retained for a total of 314 events. As mentioned by *Puleo et al.* [2000], the depiction of a swash event captured by the current meter at some distance above the bed misses the thin swash lens typically at the latter stage of backwash.

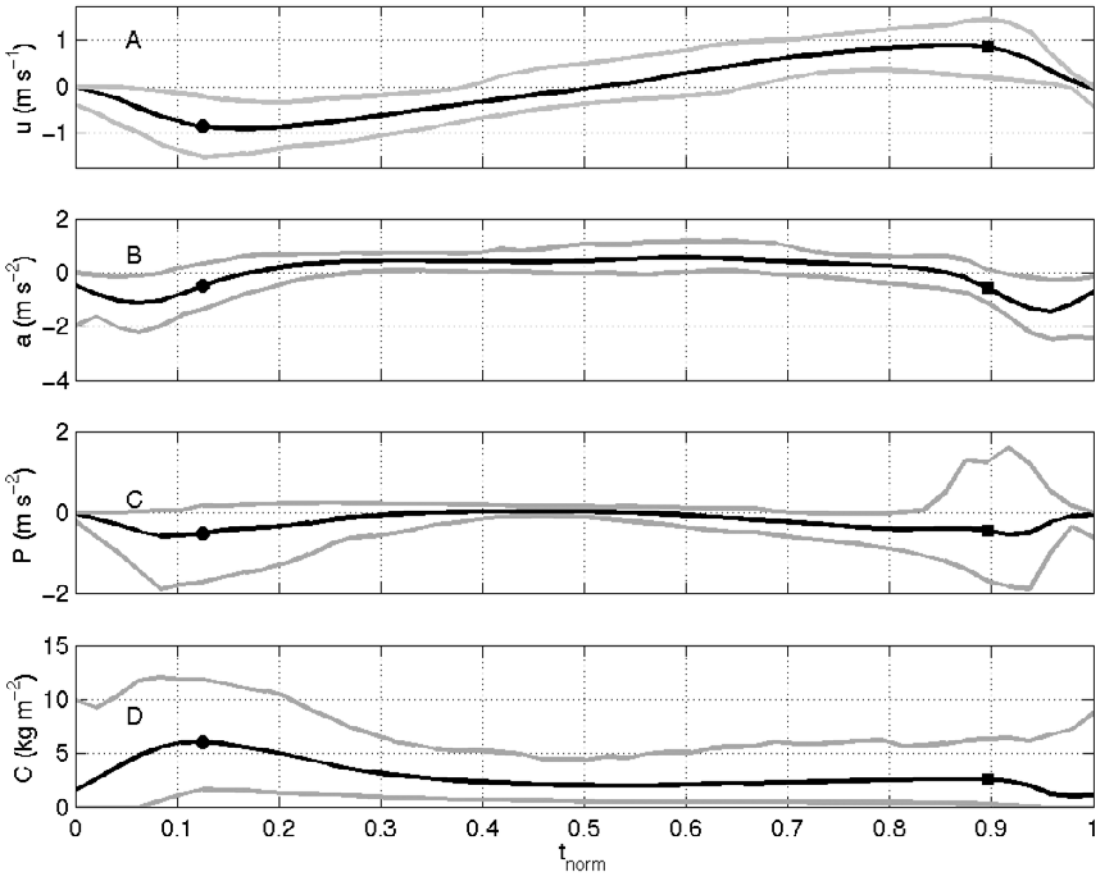

Figure 4. Ensemble average swash time (normalized) series: (a) velocity, (b) acceleration (c) horizontal pressure gradient estimate (P), and (d) suspended load. Solid circles and squares denote timing of suspended load maxima for uprush and backwash, respectively.

[23] Individual swash events were linearly interpolated to a normalized (by the duration of each swash event) time grid, t_{norm} = 0 to 1, such that ensemble averages of the measurements could be determined (Figure 4). In Figure 4a the ensemble averaged velocity time series is roughly symmetric with maximum speeds of 0.91 m s^{-1} during uprush and 0.89 m s^{-1} during backwash. The shaded lines represent the 5th and 95th percentiles of the individual events that were used for the ensemble average. The corresponding ensemble-averaged accelerations (even though the derivative process may amplify noise, we use $\langle a \rangle = \left\langle \frac{\partial u}{\partial t} \right\rangle$ rather than $\langle a \rangle = \frac{\partial \langle u \rangle}{\partial t}$; Figure 4b) show a handlebar shape similar to Figure 1, with a short-lived onshore-directed acceleration during uprush and deceleration during backwash. The acceleration magnitude ($\sim$0.5 m s^{-2}) is about half that of downslope gravity ($\sim$0.82 m s^{-2}) for the rest of the ensemble average duration. Horizontal pressure gradient estimates are roughly symmetric and largest during times of strong onshore-directed acceleration and smallest when acceleration is offshore-directed (Figure 4c). The large spread in P during the beginning and end of the cycle likely results from the estimation method since the velocity (used in Taylor's hypothesis to convert a spatial gradient to a temporal gradient) can be either positive or negative. Unlike the velocity magnitude, acceleration, and pressure gradient time series, ensemble-averaged suspended loads are asymmetric and indicate that uprush suspended loads are typically twice that of backwash suspended loads (Figure 4c). Solid circles (squares) in Figure 4 indicate the timing of the uprush (backwash) suspended load maximum. During uprush, the suspended load maximum tends to lag the acceleration magnitude maximum by 0.06 (normalized time, i.e., for a 10-s swash event, by 0.6 s or $\sim$22°) and slightly lead the velocity magnitude maximum (0.04 normalized time). Conversely, during backwash, the suspended load maximum leads the onshore-directed backwash acceleration maximum by 0.08 (normalized time) but does not lag or lead the backwash velocity maximum.

5.3. Suspended Sediment Observations

[24] Suspended load measurements from the 314 un-normalized instantaneous swash events were interpolated to an equally spaced 0.2 m s^{-1} by 0.2 m s^{-2} velocity-acceleration grid using the technique described by *Plant et al.* [2002] to show the importance of fluid acceleration (Figure 5). Since onshore flow is negative in this coordinate system, the lower left quadrant (QA) represents onshore-directed uprush acceleration (the vertical axis was clipped at -2.5 m s^{-2} because the number of observations below this cutoff was sparse causing the interpolation to have errors larger than estimated values), the upper left (QB) represents uprush deceleration, the upper right (QC) corresponds

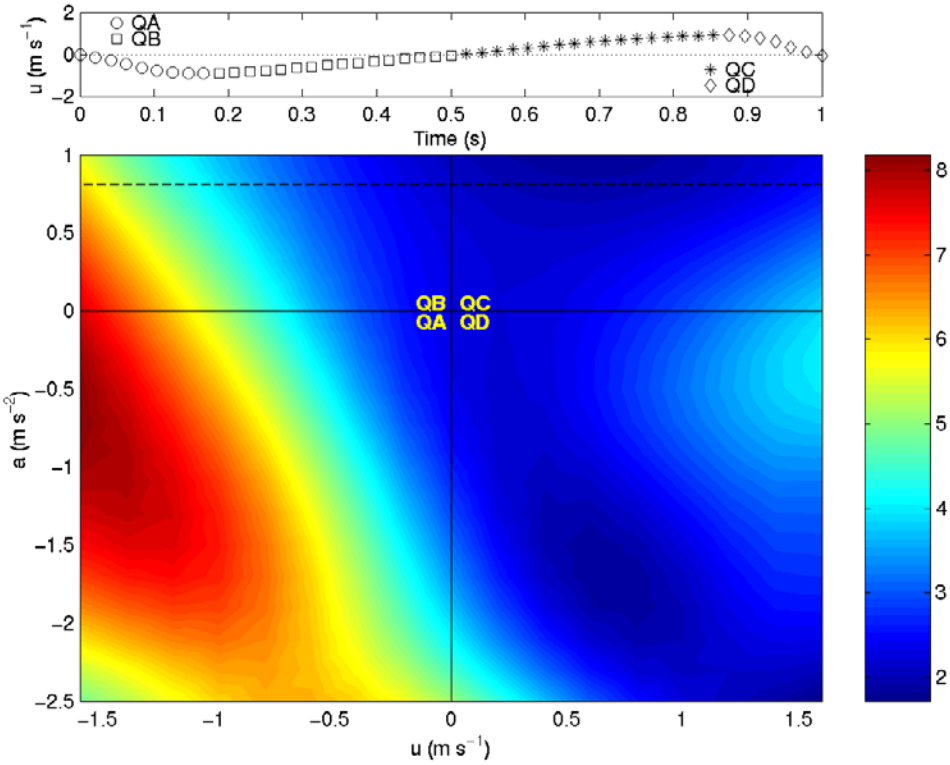

Figure 5. Interpolated suspended load (kg m^{-2}) as a function of velocity and acceleration. Dotted line is downslope gravitational acceleration and solid horizontal and vertical lines separate quadrants. Top panel shows a velocity time history of an ensemble-averaged swash event with symbols corresponding to the four quadrants.

to offshore-directed backwash acceleration, and the lower right (QD) corresponds to backwash deceleration (quadrants are separated by solid black lines). The symbols in the top panel describe the mean swash velocity time series to assist the reader in interpreting the relationship between each quadrant and the phase of swash flow. The plot shows that most of the high suspended sediment concentrations (over 7 kg m^{-2}) occur during uprush where high velocities and onshore-directed accelerations are largest. It is also clear, however, from the slopes of the color contours that for a given velocity the suspended load also increases as a function of a. In contrast, the backwash suspended loads are typically smaller at 1–3 kg m^{-2} and the largest suspended loads are confined to times when the backwash flow is decelerating.

5.4. Suspended Sediment Transport Predictions

[25] Linear regression between ensemble averages of the measured suspended sediment transport rates and predictions was performed using

$$q_B = k_b\left\langle u|u|^3\right\rangle + b_B \tag{10}$$

$$q_{pred} = k_b\left\langle u|u|^3\right\rangle + k_a\left\langle |u|^2 a\right\rangle + b_{pred}, \tag{11}$$

where angle brackets denote ensemble averaging of the time stretched values and a constant term (bias) is added to maintain the definition of the squared correlation coefficient (i.e., the model is not forced through zero). It is necessary to calculate ensemble averages in this manner (e.g. $\langle u|u|^3\rangle$ rather than $\langle u\rangle|\langle u\rangle|^3$) due to the nonlinear nature of the velocity and acceleration products. Similarly, ensemble averages of the sediment transport rates utilized $\langle uC\rangle$ rather than $\langle u\rangle\langle C\rangle$.

[26] Suspended sediment transport rate predictions indicate that the modified model more accurately predicts the timing of the uprush suspended sediment transport maximum (Figure 6a). Both models predict essentially the same maximum suspended sediment transport rate during uprush; however, the Bailard model lags the modified model. The modified model shifts the uprush peak to occur earlier in the swash cycle, more closely matching the observations. The Bailard model and the modified model are nearly coincident throughout backwash and over predict the suspended sediment transport rate by about 30%. Net predicted transport rates are roughly −445 kg s^{-2} or approximately 0.03 m^3 per m beach width per swash cycle. A very rough estimate of the predicted elevation change per swash cycle can be obtained by dividing this value by the maximum distance the swash reached beyond the sensor. Using a value of 3 m leaves 0.01 m of accretion per swash cycle. Over many cycles, this would suggest severe foreshore accretion that was not observed during this study [*Puleo et al.*, 2000]. It should be noted though, that this simple calculation incorporates only suspended load transport whereas the unmeasured bed load transport, specifically during the backwash, likely counterbalances the suspended load transport predicted during uprush.

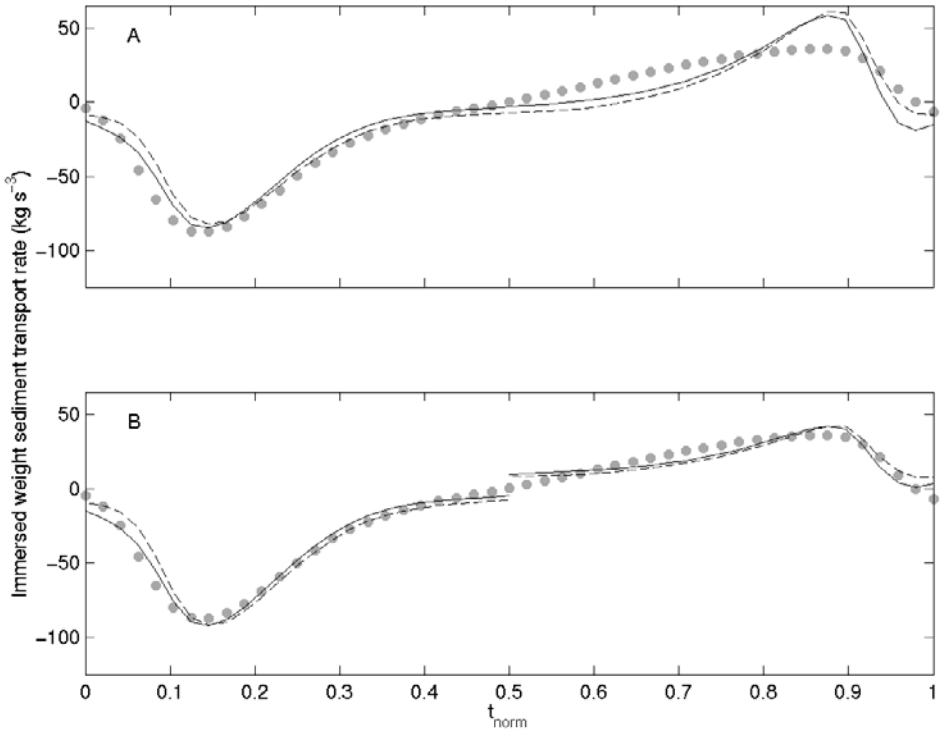

Figure 6. Suspended sediment transport rate measurements (circles) and predictions (dashed line, q_B; solid line, q_{pred}) (a) for the entire swash cycle and (b) for uprush (negative values) and backwash (positive values) portions of the swash cycle fitted separately.

[27] Coefficients (Table 1) on the first term of the Bailard or modified model have the same value of 56.0. A typically used estimate of this coefficient based on values of 1025 kg m^{-3} for ρ, 0.01 for f, 0.01 for ε_s, and 0.065 m s^{-1} for the sediment fall velocity, w, is 0.79. This estimate is 2 orders of magnitude smaller than the coefficients determined from the regression and raises concerns about the ''efficiency'' concept in the B3 models (see section 6). The constant of −8.3 for both models shows that there is a slight bias. The fact that this bias is negative means that suspended sediment transport is not predicted to occur until the velocity moment and acceleration terms reach some threshold values, analogous to the threshold criterion in a Shield's stress formulation.

[28] Although less desirable than calibrating coefficients for the entire swash cycle, the models can be split into uprush and backwash components allowing predictions and coefficients to be determined for each portion. Performing this decomposition causes the modified model to match the uprush observations both in magnitude and phase more closely (Figure 6b). During backwash, the Bailard model and modified model are again nearly coincident and match the backwash maximum more closely than in Figure 6a. Because the uprush and backwash are fit separately, there is a discontinuity in the predictions at $t_{norm} = 0.5$ for the models.

[29] One to one comparisons between the measured suspended sediment transport rates and those predicted by the models show increased correlation when the acceleration effect is included and when the models are decomposed into their uprush and backwash components (Figure 7). The R^2 value for the whole swash cycle increases from 0.90 to 0.93 for the Bailard, and modified model respectively (significant at the 99% level). In decomposing the swash cycle, the R^2 values for both the Bailard and modified model increase for the uprush portion but decrease for the backwash portion (Table 2). Because some studies have found that the energetics model using the velocity to third power had better predictive skill even for suspended sediment transport (e.g., T. Butt et al., Observations of bore turbulence in the swash and inner surf zones, submitted to *Marine Geology*, 2003) (hereinafter referred to as Butt et al., submitted manuscript, 2003), we tested equation (10) using $\langle u|u|^2\rangle$ rather than $\langle u|u|^3\rangle$ and found the R^2 value increased by only a few percent depending on whether or not it was used for the entire swash event or for the uprush or backwash decompositions. This suggests that, at least for this study, the predictive capability using the energetics model was less sensitive to the power of the velocity component than including an acceleration term.

[30] Root-mean square errors between model predictions and observations show that the inclusion of the acceleration

Table 1. Coefficients With 95% Confidence Intervals for Linear Regressions

	q_B (Bailard, No Acceleration Terms)	q_{pred} (Bailard + Acceleration Terms)
k_b, b	56.0 ± 5.4, −8.3 ± 3.4	56.0 ± 4.7, −8.3 ± 3.0
k_a,	–	9.3 ± 4.9
k_b, b uprush only	62.4 ± 6.5, −9.1 ± 4.2	60.2 ± 4.4, −10.1 ± 2.9
k_a, uprush only	–	9.7 ± 3.7
k_b, b backwash only	27.8 ± 6.5, 7.8 ± 3.8	29.4 ± 5.8, 7.0 ± 3.4
k_a, backwash only	–	5.0 ± 3.7

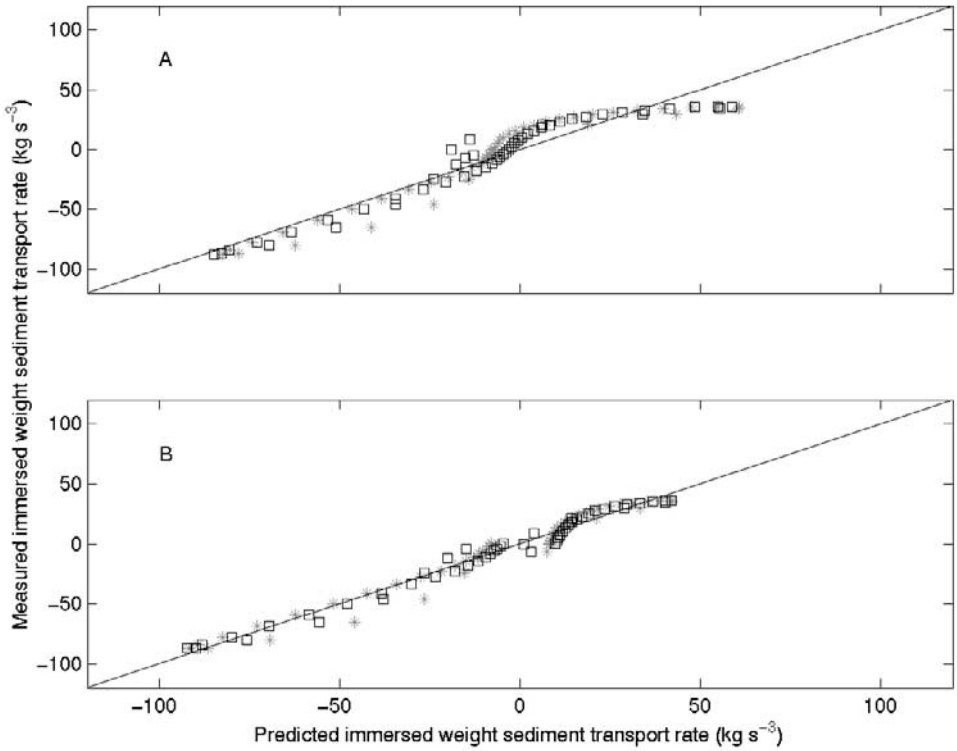

Figure 7. One to one comparison between measured suspended sediment transport rates and those predicted by (a) the Bailard model and (b) the modified Bailard model including acceleration effects. Solid line denotes perfect correlation. Shaded dots are for the entire cycle, and black dots are for values fit individually to the uprush and backwash components.

term reduces the overall error by 13%. When the ensembles are decomposed into uprush and backwash components, the error reduction becomes 35% for uprush and 14% for backwash (Table 2). The error reduction in the modified model is largely due to correcting the timing mismatch that exists between the Bailard model predictions and observations. Re-analysis using the time dependent water depth as the length scale rather than a constant value included in the regression coefficient, causes the k_a value to change but only slightly increases the correlation coefficient. Therefore, using a constant length scale did not adversely affect the predictive capability of the model.

6. Discussion

[31] Typical swash events on this steep beach display acceleration time series that are not consistent with flows governed solely by gravity and friction. Strong onshore-directed uprush acceleration and backwash deceleration that are not included in typical sediment transport models likely affect sediment transport. As a result, the Bailard model based on fluid velocities was modified to include terms accounting for the fluid acceleration. The effect of fluid acceleration is normally assumed to produce delayed boundary layer growth and hence higher velocities near the bed than flows with weaker acceleration after the same duration of boundary layer development [*King*, 1991; *Nielsen*, 1992]. In the swash zone, however, it is felt that the modification likely accounts for the disproportionate onshore-directed accelerations (as compared to backwash) observed in the shoreward propagating bore and swash front and the associated horizontal pressure gradients and not due to delayed boundary layer growth. *Nielsen* [2002] showed by theoretical arguments and field data that incorporating a phase shift in the shear stress term of a typical sediment transport model could account for the larger amount of sediment transport observed within the beginning of the uprush. *Puleo et al.* [2000] analyzed sediment transport in the swash zone bore (using this data set) and concluded that turbulent energy dissipation across the bore was a better descriptor for sediment transport across the bore than a bed

Table 2. Skill and Prediction Error for Linear Regressions

	q_B (Bailard)	q_{pred} (Bailard + Acceleration Terms)
Skill (R^2)	0.90	0.93
Skill (R^2) uprush only	0.94	0.98
Skill (R^2) backwash only	0.77	0.84
Root-mean square error (kg s^{-3})	11.5	10.0
Root-mean square error (kg s^{-3}) uprush only	7.0	4.6
Root-mean square error (kg s^{-3}) backwash only	6.2	5.3

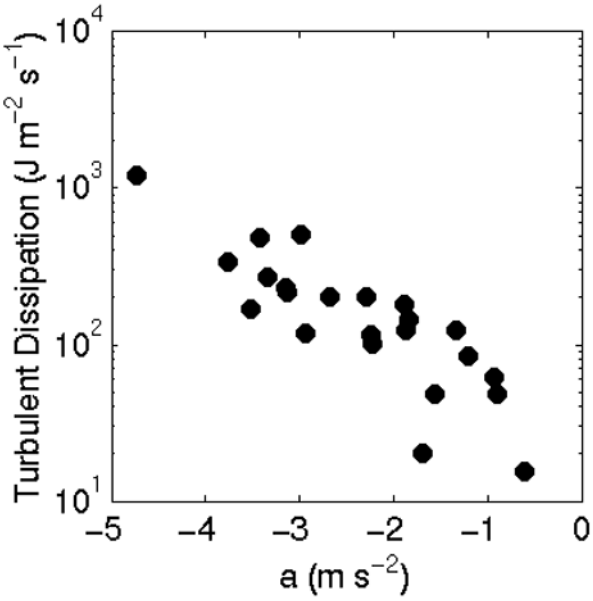

Figure 8. Turbulent bore dissipation from the bores in the *Puleo et al.* [2000] study as a function of fluid acceleration.

shear type model. Combining the statements above suggests that the bore dissipation and fluid acceleration may be related. For instance, the bore dissipation observations from *Puleo et al.* [2000] are plotted against the fluid acceleration and show that the two fluid descriptors are related (Figure 8). While this figure does not prove that turbulent dissipation and acceleration are interchangeable, it does show that using the acceleration modification may account for the turbulent bore dissipation in a proxy form.

[32] The rather high R^2 values observed in this study, even for the Bailard model, seem to contradict the findings by *Puleo et al.* [2000] using this same data set. In that study, it was found that the bed shear type model was typically a poorer predictor of observed sediment transport rates (maximum R^2 was 0.6), whereas this study showed that with or without an acceleration modification, the Bailard model more accurately predicted suspended sediment transport. The difference between the two studies is important. The present study used ensemble averages of a set of swash events, so that the aim was to predict a time dependent sediment transport rate for an ''average'' swash event and determine the effect of fluid acceleration from a typical swash event on suspended sediment transport. The prior study by *Puleo et al.* [2000] analyzed the bed shear type model for instantaneous and time averaged transport which is different from ensemble averaging unless every swash event is nearly identical. Nevertheless, re-analysis of the data in the *Puleo et al.* [2000] study but using the acceleration term incorporated here slightly increased the R^2 value.

[33] Since backwash flows are mostly controlled by gravity and friction, it would have been expected that offshore-directed accelerations would be important to backwash suspended sediment transport similar to onshore-directed uprush accelerations. It has been shown that long duration backwashes, presumably able to reach near gravity acceleration are effective at suspending and transporting sediment [*Butt and Russell*, 1999; *Puleo et al.*, 2000; *Holland and Puleo*, 2001; *Butt et al.*, 2002]. The sensor location in the upper swash zone during this study meant that many of the observed swashes were of short (<8 s) duration implying that long duration backwashes were not observed and may have masked the importance of offshore-directed accelerating backwash. Accelerating backwash flow, however, is also thinning in its seaward retreat, and potentially hampers the acceleration effect on suspended sediment transport. Because the flow is thinning, there is less water column to suspend sediment and it is likely that during much of the backwash flow sediment is transported as bed load [*Horn and Mason*, 1994] or sheet flow. Hence an offshore-directed acceleration (as opposed to deceleration) effect cannot be confirmed or contradicted with data from this study.

[34] It was observed that decelerating backwash (Figure 5; QD) had larger sediment transport rates than did accelerating backwash (Figure 5; QC) at a given velocity. This implies that some mechanism is entraining more sediment during this latter portion of backwash. When the backwash is decelerating, it must be acted upon by an adverse pressure gradient and to a lesser extent friction, since gravity is acting to accelerate the flow. The decelerating backwash often collides with the next uprush resulting in a hydraulic jump or backwash vortex that has been shown to be an effective suspending mechanism [*Matsunaga and Honji*, 1980; *Butt et al.*, 2002] and may help explain the large values observed here. Also, *Hanes and Huntley* [1986] suggested that boundary layer separation during decelerating flow may be associated with sediment suspension.

[35] Although the notions of hydraulic jumps and boundary layer separation could not be readily investigated with this data set, the suggestion by *Hanes and Huntley* [1986] that boundary layer separation may be associated with sediment suspension can be addressed through horizontal pressure gradients since boundary layer separation can occur under conditions of an adverse pressure gradient. It was shown that during decelerating backwash, when backwash suspended sediment transport was largest, the horizontal pressure gradient estimate was large and onshore-directed (Figure 4), consistent with the notion of an adverse pressure gradient. Other studies have also shown that strong horizontal pressure gradients at the bed are able to influence sediment transport [e.g., *Drake and Calantoni*, 2001]. Thus it is felt that suspended sediment transport during decelerating backwash is likely enhanced by these mechanisms (hydraulic jump/backwash vortex, boundary layer separation and adverse pressure gradients), but warrants further investigation.

[36] While the Bailard model had high R^2 values regardless of whether or not it was used for the entire swash cycle or for the uprush and backwash portion individually, several inadequacies may exist. First, the k_B coefficients were large and implied an efficiency factor of about 0.7. Similar to previous studies [*Masselink and Hughes*, 1998; *Puleo et al.*, 2000; *Drake and Calantoni*, 2001] the efficiency factor was predicted to be more than an order of magnitude larger than typically used values. Therefore it is likely that if the B3 type model is accepted for the swash zone, the efficiency factor for these highly turbulent, time-dependent flows must be necessarily larger than the originally proposed value for time averaged flows [*Bagnold*, 1963, 1966], or it may suggest that the use of an efficiency factor in the sediment

transport formulation is undesirable. Second, the B3 type model, assumes that instantaneous sediment transport rates are a function of instantaneous flow conditions. Because of this assumption, pre-suspended sediment advection (from the inner surf zone or the bore) is not accounted for. Unfortunately, in the swash zone, where hydraulic jumps and bore collapse appear to be dominant sediment suspending mechanisms, the exclusion of advected sediment and water column storage of sediment [*Kobayashi and Johnson*, 2001] should be expected to cause errors in the B3 approach. Studies by *Puleo et al.* [2000] and Butt et al. (submitted manuscript, 2003), however, showed that sediment tends to settle out quickly behind the shoreward propagating bore such that the lack of pre-suspended sediment advection in the B3 type swash zone sediment transport model may not represent a significant source of error.

7. Conclusion

[37] Suspended sediment concentrations and fluid velocities collected in the swash zone of a high energy, steep beach showed that high values of suspended sediment concentration (over 7 kg m^{-2}) were observed during times of rapid velocities, uprush acceleration and onshore directed pressure gradients during uprush associated with the shoreward propagating bore. Maximum suspended sediment concentrations reached 3 kg m^{-2} during backwash but occurred during decelerating flow, when the backwash is likely slowed by adverse pressure gradients from the ensuing uprush. An energetics model for sediment transport was modified to include the effect of fluid acceleration and was able to reduce the root-mean square prediction error by up to 35% over the energetics model without the modification suggesting that the inclusion of the acceleration term may account for the additional sediment transporting mechanisms during the unsteady flow conditions observed in the swash zone.

[38] **Acknowledgments.** J. A. P., K. T. H. and N. G. P. were supported by the Office of Naval Research (ONR) through base funding to the Naval Research Laboratory (PE#61153N). DNS was supported by ONR (grant N00014-01-1-0152). We thank Rob Holman and Reggie Beach for allowing us to utilize the Gleneden data set and Joe Calantoni for his comments.

References

Admiraal, D. M., M. H. Garcia, and J. F. Rodriguez, Entrainment response of bed sediment to time-varying flows, *Water Resour. Res.*, *36*(1), 335–348, 2000.

Bagnold, R. A., Mechanics of marine sedimentation, in *The Sea*, edited by M. N. Hill, pp. 507–528, Wiley-Intersci., Hoboken, N. J., 1963.

Bagnold, R. A., An approach to the sediment transport problem from general physics, report, 37 pp., U.S. Geol. Surv., Washington, D. C., 1966.

Bailard, J. A., An energetics total load sediment transport model for a plane sloping beach, *J. Geophys. Res.*, *86*(C11), 938–954, 1981.

Beach, R. A., and R. W. Sternberg, Infragravity driven suspended sediment transport in the swash, inner and outer-surf zone, in *Coastal Sediments '91*, edited by N. C. Kraus, K. J. Gingerich, and D. L. Kriebel, pp. 114–128, Am. Soc. of Civ. Eng., Seattle, Wash., 1991.

Bowen, A. J., Simple models of nearshore sedimentation: Beach profiles and longshore bars, in *The Coastline of Canada*, edited by S. B. McCann, pp. 1–11, Geol. Surv. of Can., Ottawa, Ont., Can., 1980.

Butt, T., and P. Russell, Suspended sediment transport mechanisms in high-energy swash, *Mar. Geol.*, *161*(2–4), 361–375, 1999.

Butt, T., P. Russell, and I. Turner, The influence of swash infiltration-exfiltration on beach face sediment transport: Onshore or offshore?, *Coastal Eng.*, *42*(1), 35–52, 2001.

Butt, T., P. Russell, G. Masselink, J. Miles, D. Huntley, D. Evans, and P. Ganderton, An integrative approach to investigating the role of swash in shoreline change, paper presented at 28th International Conference on Coastal Engineering, Am. Soc. of Civ. Eng., Cardiff, Wales, 2002.

Butt, T., P. Russell, J. A. Puleo, J. Miles, and G. Masselink, Observations of bore turbulence in the swash and inner surf zones, *Marine Geology*, submitted.

Cowen, E. A., I. M. Sou, P. L.-F. Liu, and B. Raubenheimer, PIV measurements within a laboratory generated swash zone, *J. Eng. Mech.*, *129*, 1119, 2003.

Drake, T. G., and J. Calantoni, Discrete particle model for sheet flow sediment transport in the nearshore, *J. Geophys. Res.*, *106*(C9), 19,859–19,868, 2001.

Elgar, S., E. L. Gallagher, and R. T. Guza, Nearshore sandbar migration, *J. Geophys. Res.*, *106*(C6), 11,623–11,627, 2001.

Gallagher, E. L., S. Elgar, and R. T. Guza, Observations of sand bar evolution on a natural beach, *J. Geophys. Res.*, *103*(C2), 3203–3215, 1998.

Hanes, D. M., and D. A. Huntley, Continuous measurements of suspended sand concentration in a wave dominated nearshore environment, *Cont. Shelf Res.*, *6*(4), 585–596, 1986.

Hardisty, J., J. Collier, and D. Hamilton, A calibration of the Bagnold beach equation, *Mar. Geol.*, *61*(1), 95–101, 1984.

Ho, D. V., and R. E. Meyer, Climb of a bore on a beach: 1. Uniform beach slope, *J. Fluid Mech.*, *14*(20), 305–318, 1962.

Hoefel, F., and S. Elgar, Surfzone sandbar migration and wave acceleration induced sediment transport, *Science*, *299*, 1885, 2003.

Holland, K. T., and J. A. Puleo, Variable swash motions associated with foreshore profile change, *J. Geophys. Res.*, *106*(C3), 4613–4623, 2001.

Horn, D. P., and T. Mason, Swash zone sediment transport modes, *Mar. Geol.*, *120*(3–4), 309–325, 1994.

Hughes, M. G., G. Masselink, and R. W. Brander, Flow velocity and sediment transport in the swash zone of a steep beach, *Mar. Geol.*, *138*(1–2), 91–103, 1997.

Jaffe, B. E., and D. M. Rubin, Using nonlinear forecasting to learn the magnitude and phasing of time-varying sediment suspension in the surf zone, *J. Geophys. Res.*, *101*(C6), 14,283–14,296, 1996.

Johnson, R. S., *A Modern Introduction to the Mathematical Theory of Water Waves*, 445 pp., Cambridge Univ. Press, New York, 1997.

King, D. B. J., Studies in oscillatory flow bedload sediment transport, Ph.D. thesis, Univ. of Calif., San Diego, San Diego, Calif., 1991.

Kirkgöz, M. S., A theoretical study of plunging breakers and their run-up, *Coastal Eng.*, *5*(4), 353–370, 1981.

Kobayashi, N., and B. D. Johnson, Sand suspension, storage, advection, and settling in surf and swash zones, *J. Geophys. Res.*, *106*(C5), 9363–9376, 2001.

Masselink, G., and M. Hughes, Field investigation of sediment transport in the swash zone, *Cont. Shelf Res.*, *18*(10), 1179–1199, 1998.

Matsunaga, N., and H. Honji, The backwash vortex, *J. Fluid Mech.*, *99*(AUG), 813–815, 1980.

Meyer-Peter, E., and R. Muller, Formulas for bed-load transport, paper presented at 3rd Meeting, Int. Assoc. for Hydraul. Res., Delft, Netherlands, 1948.

Nielsen, P., *Coastal Bottom Boundary Layers and Sediment Transport*, 324 pp., World Sci., River Edge, N. J., 1992.

Nielsen, P., Shear stress and sediment transport calculations for swash zone modelling, *Coastal Eng.*, *45*(1), 53–60, 2002.

Osborne, P. D., and G. A. Rooker, Sand re-suspension events in a high energy infragravity swash zone, *J. Coastal Res.*, *15*(1), 74–86, 1999.

Petti, M., and S. Longo, Turbulence experiments in the swash zone, *Coastal Eng.*, *43*(1), 1–24, 2001.

Plant, N., K. T. Holland, and J. A. Puleo, Analysis of the scale of errors in nearshore bathymetric interpolation, *Mar. Geol.*, *191*, 71–86, 2002.

Puleo, J. A., and K. T. Holland, Estimating swash zone friction coefficients on a sandy beach, *Coastal Eng.*, *43*(1), 25–40, 2001.

Puleo, J. A., R. A. Beach, R. A. Holman, and J. S. Allen, Swash zone sediment suspension and transport and the importance of bore-generated turbulence, *J. Geophys. Res.*, *105*(C7), 17,021–17,044, 2000.

Shen, M. C., and R. E. Meyer, Climb of a bore on a beach: 3. Run-up, *J. Fluid Mech.*, *16*(8), 113–125, 1963.

Thornton, E. B., R. T. Humiston, and W. Birkemeier, Bar/trough generation on a natural beach, *J. Geophys. Res.*, *101*(C5), 12,097–12,110, 1996.

D. M. Hanes, and D. N. Slinn, University of Florida, Civil and Coastal Engineering Department, Gainesville, FL 32611-6590, USA. (dhanes@usgs.gov; slinn@coastal.ufl.edu)

K. T. Holland, N. G. Plant, and J. A. Puleo, Naval Research Laboratory, Code 74403, Stennis Space Center, MS 39529, USA. (tholland@nrlssc.navy.mil; nplant@nrlssc.navy.mil; jpuleo@nrlssc.navy.mil)